SCIENTIFIC CULTURE

www.sci-cult.com

*SCIENTIFIC CULTURE, Vol. 12, No. 2.1, (2026), pp. 3849-3864*
*Open Access. Online & Print*

**DOI: 10.5281/zenodo. 18866687**

# CHARACTERIZATION OF CLAYS FROM BOYACÁ (COLOMBIA) WITH POTENTIAL CERAMIC USE

**Nubia Edith Céspedes Prieto[1], Jesús Sigifredo Valencia Ríos[2], Juan Bautista Carda Castelló[3]**

*[1]Escuela de Ingenieros Militares, Ejército Nacional de Colombia, Bogotá D.C., Colombia. Email: necespedesp@unal.edu.co, https://orcid.org/0000-0002-5248-3898, Escola Superior de Ceràmica de L'Alcora, L´Alcora, España*
*[2]Universidad Nacional de Colombia, Laboratorio de Catálisis Heterogénea, Departamento de Química, Facultad de Ciencias, Bogotá D.C., Colombia. Email: jsvalenciar@unal.edu.co, https://orcid.org/0000-0002-2171-7006*
*[3]Universitat Jaume I de Castelló, Grupo de Investigación de Química del Estado Sólido, Cátedra de Innovación Cerámica "Ciutat de Vila–Real", Departamento de Química Inorgánica y Orgánica, Castellón de la Plana, España*

*Received: 21/12/2025*
*Accepted: 13/02/2026*

## ABSTRACT

***The region of Boyacá (Colombia) features an important variety of mining resources, including clay minerals, siliceous sands, diatomite, quartz, limestone and phosphoric rock, among others. In this investigation, the clays present in the municipalities of Sogamoso, Ráquira and Cómbita are very important, given their strong potential for ceramic use (v. gr. Ceramic tiles). The studies are developed through mineralogical analysis via X-ray diffraction, chemical composition via X-ray fluorescence and an evaluation of physical–chemical properties such as linear contraction, porosity and mechanical resistance, considered priority information to develop applications in the field of ceramic science and technology (i.e., porcelain stoneware).***

**KEYWORDS:** Clay minerals, Clays, Ceramic materials, Gresification.

## 1. INTRODUCTION

Humans have made objects from terracotta (modeled and hardened clay) since ancient times. Some examples are the statuettes of Mohenjo-Daro (Pakistan)1 and ceramic items located in the Middle East and Anatolia.2 Pottery, defined as the art of making articles from moistened clay (mud), such as figures, plates, vessels, bricks, tiles, earthenware and porcelain, also has very ancient origins dating back to the Upper Paleolithic (Gravettian period). The subsequent invention and profusion of pottery objects that spread in the Neolithic period coincided with the expansion of agriculture.3 The production of clay objects and utensils, which are subjected to firing at high temperatures after drying, is also called ceramics. Although ceramics and pottery are synonyms, ceramics are usually associated with hard, sintered nonmetallic solids, decorated articles, coatings, flooring, refractories, colored objects or enameled products that, in addition to clay, incorporate kaolin, feldspars, pozzolans and other minerals.4,5

Traditional ceramics are materials prepared from clays, which, in raw form, are made up of at least 20% of clay minerals. Geologically, clays, primarily (residual) and secondary (drag), are fragmented sedimentary rocks with particle sizes less than 3.9 □m, which are part of the soil mixed with quartz, plagioclase, feldspars, pyroxenes, oxides of titanium, limonite and carbon.6 From a chemical point of view, clays are aggregates of hydrated aluminosilicates, more specifically hydrated aluminum phyllosilicates that incorporate small amounts of iron, alkali ions and alkaline earth metals, as well as carbonates, sulfates, halides and phosphates.7 One of the important characteristics of clays is their ability to retain water, which gives them a plastic consistency that makes them moldable.8 Once dehydrated and cooked, rigid and strong bodies are obtained.

Clayey sediments, which can be found in outcrops or in deposits (reservoirs), are widely distributed in the lithosphere. Therefore, clays are diverse in composition and properties; they contain kaolinite, alumina, iron and other clay minerals, such as halloysite, illite and montmorillonite. The applications of these minerals depend on the abundance of kaolinite, the alumina content and the presence of iron, which gives color to the green or fired pieces.9

Understanding the nature and behavior of clay minerals involves the classification of clays, which is performed on the basis of chemical composition, interlaminar distance, and crystallographic symmetry. The representative unit of phyllosilicates is the tetrahedral group $SiO_4^{4-}$, which extends through siloxane bridges, forming layers of the formula $(Si_2O_5)_n^{2n-}$. In the mineral gibbsite, the structural unit is the $AlO_6^{6-}$ group, which is octahedral and extends to form layers. An identical situation occurs in brucite, a magnesium mineral whose formula is $MgO_6^{6-}$. In phyllosilicates, tetrahedral layers can join octahedral layers (type gibbsite or brucite) to form structures T:O (1:1 sheets, bilaminar), T:O:T (2:1 sheets, trilaminar), T:O:T:O:T:OT (plates 2:1:1) and O: T:O (plates 2:1, inverted).10

The organization of the phyllosilicates in layers determines the classification of the lamellar groups. The main lamellar groups are kaolin and serpentine, talc and pyrophyllite, smectites (montmorillonite and saponite), vermiculite, micas, chlorites, and sepiolite and palygorskite (atapulgite).11 Additionally, if one of every three octahedral positions is free and the rest are occupied by $Al^{3+}$ or $Fe^{3+}$ in the gibbsite-type layer, the sheet is dioctahedral. If all the octahedral sites in the brucite-type layer are occupied with $Mg^{2+}$ (or $Fe^{2+}$), the sheet is trioctahedral. In the different mineralogical groups, the ordered sheets appear to be stacked; then, the interlaminar distance is measured from the exposed surface of the tetrahedral (outer) layer to the inner face of the next tetrahedral sheet. In this way, the characteristic separations are 7.0 Å for the clays of the 1:1 lamellar group, from 9.0 to 15.0 Å for the clays of the 2:1 group, and 14 Å for the clays of the 2:1:1 group.

In practice, the technological use of common clays (miscellaneous), special clays (smectites and hormites) and kaolins (primary and residual) involves the prior identification and classification of clay minerals.12 However, regarding the technical applications of clay minerals, a traditional classification persists that is based on a predominant laminar group of kaolins (residual clay located in situ), plastic clays (carried: alluvial, lacustrine, marine, estuarine sandstones, glacial and aeolian), refractory clays, high alumina clays, plastic bond clays, brick clays, montmorillonites (fuller earth and bentonites), halloysites, and attapulgite, among others (micas, illites, allophanes).

In recent decades, the manufacture of clay-based ceramic coverings and floors, which produces tiles with different features and functionalities, has become one of the areas with the greatest impact in the fields of science and technology focused on construction materials.13 Ceramic processing with clay minerals involves operations related to grinding and adapting raw materials, mixing, adding water

and dispersants or binders, granulation, shaping (pressing, extrusion, and casting), drying, glazing, decorating and firing. Good manufacturing practices are required for mitigating environmental impacts and sustainable development in the face of the rational use of water resources and energy. Thus, prospecting and exploiting clay minerals with potential ceramic applications are tasks that require research and knowledge.

The main purpose of this work is to carry out chemical, mineralogical and thermal characterization of clay minerals collected from existing outcrops in the central region of the Department of Boyacá (Colombia) to establish formulations for the manufacture of ceramic pavements (red porous, porous white) and porcelain stoneware.

## 2. EXPERIMENTAL

Clay minerals were collected in the towns of Ráquira, Duitama and Sogamoso in the Department of Boyacá (Colombia). Outcrops of sedimentary and folded rocks from the Cretaceous period predominate in this area and are composed of shale and sandstone, as well as compact rocks such as limestone. The samples were dried in the shade at room temperature, broken down via gentle grinding, and the rocks and plant material were separated.

The clays were dried at 110 °C for 12 hours in an air atmosphere; they were then ground in a ball mill, Model Speedy–N (Nanetti, Faenza, Italia) and passed through a No. 230 U. S. Standard Sieve Series, 63 □m opening (W. S. Tyler, Mentor, USA). The apparent density was determined by pycnometry. The plasticity of the clay minerals14 was determined according to the Pffeferkorn method in a Plasticimeter (Nanetti, Faenza, Italy).

Chemical analysis was performed via X-ray fluorescence (XRF). For this purpose, an exactly weighed sample of the dry mineral was mixed with boric acid using a ball mill; the sample holder was filled with the solid, compacted at 150 bars in an automated bench press (Carver, Wabash, USA) and then taken to the analytical chamber of a Bruker S4 Pioneer sequential spectrometer (Bruker, Billerica, USA). The total carbonate content was determined by titration, in which the excess of hydrochloric acid (analytic grade, Merck KGaA, Darmstadt, Germany) was titrated with a sodium hydroxide (analytic grade, Merck KGaA, Darmstadt, Germany) solution in the presence of bromothymol blue (indicator, Sigma–Aldrich, Saint Louis, USA).

The mineralogical analysis consisted of determining the presence of laminar clay groups via X-ray diffraction (XRD) by the powder method with a Bruker AXS diffractometer, Model D4 Endeavor (Bruker, Billerica, USA), equipped with a copper anode (line K□, □ = 1.5405 Å), with a scanning angle of 0.1 at 2□ degrees and a duration of 3 s.

The thermal, differential and gravimetric analyses, in an air atmosphere, were carried out in a Marc–Bähr simultaneous thermal analyzer (ATD/ATG), model STA 503 (BÄHR-Thermoanalyse, Hüllhorst, Germany) with a ramp of 5 K min–1, between room temperature and 1200 °C.

To prepare the slips, 600 g of dry clay mineral were weighed, 0.70% of sodium metasilicate (analytic grade, Merck KGaA, Darmstadt, Germany) and 0.20% of sodium tripolyphosphate (technical grade 85%, Sigma–Aldrich, Saint Louis, USA) as deflocculants, and 300 g of distilled water were added. The mixture was taken to a PM 100 planetary mill (Retsch, Haan, Germany) and stirred for 4 to 6 minutes, dried at 110 °C for 12 hours and ground to obtain a micronized powder. The micronized solid was weighed, enough water was added to obtain a humidity of 5.5–6.0%, homogenized and passed through a 140 U. S. Standard Sieve Series, 106 □m opening (W. S. Tyler, Mentor, USA). With the micronized material, the samples were prepared in cylindrical molds at 500 kg cm–2 in an bench top automated press (Carver, Wabash, USA) maintaining pressure for 5 s. The samples were dried at 110 °C for 3 h and then cooked in an air atmosphere at temperatures between 1090 and 1165 °C for 1 hour. The fired pieces were subjected to "black heart" analysis and measurements of apparent density, linear shrinkage and water absorption capacity.

The apparent density of the raw (dried) and cooked samples was obtained from the mass and dimensions of each sample, which were determined with a Vernier-type caliper (Mitutoyo, Aurora, USA); this same information was used to establish linear shrinkage. To evaluate the water absorption capacity, the boiling method was used; for this purpose, the masses of the cooked and cooled samples (in a desiccator) were recorded; then, the samples were placed in a chamber with boiling distilled water for a period of 60 min; the heat was suspended, and the samples were allowed to cool to extract, dry (with a wet dryer) and weigh.15 The so-called scale diagrams are constructed by putting the temperature on the abscissa (x) and the water absorption (%) or linear contraction (%) on the ordinate (y).

The color of the fired pieces, at laboratory temperature, was determined in a CIELAB in a colorimeter model CR–5 (Konica Minolta, Tokyo, Japan). The apparent color of the ceramic pieces was compared with Pantone systems (Pantone Inc.,

Carlstadt, USA).

## 3. RESULTS AND DISCUSSION

### *3.1. Chemical Composition*

Clays are mixtures, in variable proportions, of clay minerals whose chemical structure consists of hydrated aluminosilicates of the phyllosilicate family (dioctahedral and trioctahedral). They are classified into 7 mineralogical groupings, among which, with reference to the highest content of alumina, the kaolin and serpentine groups stand out. They have 1:1 (T:O) sheets and contain kaolinite, dickite, chrysotile and antigorite as representative minerals. Considering that clay minerals result from the hydrothermal degradation of feldspars, kaolinite is a phyllosilicate that has the formula Al2O3.2SiO2.2H2O; thus, the "ideal" composition of kaolinite is 39.50% alumina and 46.54% silica, with an Al2O3/SiO2 molar ratio of 0.50.

Table 1 shows the chemical compositions of the clays from the department of Boyacá (Colombia), which were obtained via X-ray fluorescence and expressed in oxides. These clays contain mainly SiO2 and Al2O3, which make up the phyllosilicates, with contributions from quartz, silica and gibbsite. Additionally, alkaline oxides (Na2O and K2O), alkaline earth oxides (MgO and CaO, which in addition to being incorporated into the brucite layer, can be found as carbonates and hydroxycarbonates), refractory oxides (TiO2 and, in some cases, MnO), sulfates and sulfides (expressed as SO3) and phosphates (estimated as P2O5) stand out.

***Table 1: Characteristic chemical composition of clays from the Department of Boyacá (Colombia).***

| Clay | $Na_2O$ | MgO | $Al_2O_3$ | $SiO_2$ | $P_2O_5$ | $SO_3$ | $K_2O$ | CaO | $TiO_2$ | MnO | $Fe_2O_3$ | BL |
|---|---|---|---|---|---|---|---|---|---|---|---|---|
| **Sogamoso 1 (S1)** | 0.02 | 0.64 | 19.79 | 56.63 | 0.31 | 0.99 | 1.78 | 0.21 | 1.03 | 0.02 | 7.62 | 10.98 |
| **Sogamoso 2 (S2)** | 0.09 | 0.42 | 18.76 | 65.95 | 0.12 | 0.02 | 0.79 | 0.16 | 0.65 | 0.00 | 2.45 | 10.66 |
| **Sogamoso 3 (S3)** | 0.09 | 0.17 | 11.87 | 80.07 | 0.04 | 0.06 | 0.31 | 0.10 | 0.54 | 0.00 | 0.87 | 5.96 |
| **Cómbita 1 (C1)** | 0.21 | 0.22 | 21.81 | 56.90 | 0.11 | 0.13 | 0.97 | 0.19 | 1.09 | 0.01 | 4.56 | 6.60 |
| **Cómbita 2 (C2)** | 0.18 | 0.21 | 26.99 | 59.02 | 0.09 | 0.03 | 1.23 | 0.04 | 1.27 | 0.00 | 0.83 | 10.29 |
| **Cómbita 3 (C3)** | 0.28 | 0.44 | 22.09 | 60.90 | 0.07 | 0.07 | 1.02 | 0.17 | 0.95 | 0.01 | 4.65 | 9.63 |
| **Cómbita 4 (C4)** | 0.40 | 0.17 | 15.41 | 73.84 | 0.11 | 0.03 | 0.60 | 0.05 | 1.24 | 0.00 | 2.60 | 5.95 |
| **Cómbita 5 (C5)** | 0.15 | 0.32 | 18.23 | 69.68 | 0.11 | 0.02 | 0.80 | 0.11 | 0.88 | 0.00 | 2.86 | 7.00 |
| **Ráquira 1 (R1)** | 0.14 | 0.16 | 20.73 | 63.47 | 0.13 | 0.03 | 0.79 | 0.10 | 1.19 | 0.00 | 4.56 | 8.85 |
| **Ráquira 2 (R2)** | 0.28 | 1.16 | 20.72 | 55.99 | 0.12 | 0.07 | 1.49 | 0.81 | 1.00 | 0.03 | 7.53 | 11.08 |
| **Ráquira 3 (R3)** | 0.24 | 0.37 | 17.21 | 67.75 | 0.14 | 0.04 | 1.08 | 0.13 | 0.81 | 0.03 | 5.67 | 6.76 |
| **Ráquira 4 (R4)** | 0.09 | 0.34 | 24.16 | 57.80 | 0.16 | 0.03 | 0.61 | 0.15 | 1.18 | 0.01 | 3.99 | 11.57 |

**BL = Burning losses. In brackets, the simplified clay designation. All data in percentages.**

The amount of chromophore oxides, such as Fe2O3, varies between 0.83% for the "Cómbita 1" clay and 7.62% for the "Sogamoso 1" clay. The TiO2 content of the rutile variety varies between 0.54% for the "Sogamoso 3" clay and 1.27% for the "Cómbita 2" clay. Iron oxide results in a red color, whereas titanium oxide (rutile) results in a yellow tone.

In all the cases, the sum of alkaline oxides does not exceed 1.80%; likewise, the presence of alkaline earth oxides (e.g., MgO + CaO) does not exceed 1.80%. This means that, technically, these clays can exceed the expectation of brick making in favor of more technical ceramic applications. On the other hand, it was verified that all clays contain minimal amounts of total carbonate, suggesting the need to add limestone to ceramic preparations. The calcination losses are relatively high (ranging between 5.95% for clay C4 and 14.02% for sample C1), which is explained by the fact that, during the thermal treatment, in an air atmosphere, the combustion products of organic matter and crystallization water are lost and released as a consequence of the dehydroxylation of the aluminosilicates.

In all the clays examined, the alumina content is relatively high, with S3 (with 11.87%) being the solid with the lowest Al2O3 content. Despite these results, which correspond to high-quality clays, with the exception of C2 clay, which contains 26.99% Al2O3, with 0.83% Fe2O3, and with a sum of Na2O and K2O that reaches 1.31%, none of the materials examined can be classified as "refractory clay" since the solids do not have the ability to sinter at low temperatures. For C2 clay, it is necessary to verify that the excess SiO2 does not affect the pyrometric cone and that it is above 1600 °C. Additionally, in terms of the Al2O3 content, none of the clays are "high alumina", which suggests the absence of gibbsite and boehmite.

Table 1 shows that all the clays examined in this

work exceed the theoretical content of SiO2 with respect to kaolinite (which is 46.54%). The SiO2 content fluctuates between 55.99% (R2 clay) and 80.07% (Sogamoso 3 clay). The high silicon oxide content in clays S2, S3, C4, C5, and R3, which exceeds 65.00%, is largely due to the presence of quartz sands. Likewise, in no case does the alumina composition exceed 27.00%. Clays C2 (with 26.99%) and R4 (with 24.16%) have the highest alumina content; therefore, although a high refractory capacity is assumed, from this perspective, no solid can be classified as "white clay". After firing, the white tones represent, in raw form, a content of (Fe2O3 + TiO2) less than 1.0%, which none of the clays meet.

The visualization of the molar ratio (Al2O3/SiO2) on the basis of the sum of the oxides (M2O + MO + Fe2O3) provides a "guiding criterion" for the eventual technological grouping of clays (Augustinik's diagram).16 Thus, the maximum molar ratio (Al2O3/SiO2) is 0.27 (C2 clay), which is well below a ratio of 0.40, from which refractory clays are located; the minimum ratio is 0.09, which is suitable for clays for clinkering pavements and bricks. Many of the ratios (Al2O3/SiO2) are between 0.15 and 0.25, which are clays used for pottery and terracotta. In summary, the high content of SiO2 and the low content of fluxing oxides hinder the application of these clays in the production of tiles, ducts and artificial stones without the addition of alumina or flux improvers.

Plasticity is among the best characteristics of clays; owing to this property, which essentially depends on the amount of water surrounding the particles, it is possible to mold clays. Certain sedimentary clay minerals, v. gr. from the 2:1 group or the (2:1):1 group, such as smectites, tend to absorb more water than those from the 1:1 group (kaolinites and serpentines); thus, plasticity has a certain relationship with the proportion of "expandable and nonexpandable" minerals in the clay. However, the plastic characteristics of clays17 depend not only on the water content but also on factors associated with the particles (size, shape, structure, orientation, state of aggregation and surface area) and the existence of organic matter, occluded gases, electrolytes, flocculating substances, and thermal treatment, which promote dehydration and sintering.

In all the clays examined, the presence of phosphorus, determined as P2O5, stands out. In addition to silicate ions (SiO3=) and oxalate (C2O4=), it is possible to use different phosphates (hexametaphosphate, tripolyphosphate and pyrophosphate) as deflocculating agents, which can adsorb on the surface of colloidal particles, dispersing them and increasing their fluidity by decreasing their viscosity.18,19,20,21,22 Depending on the nature of the clays, typical deflocculant loadings range between 0.15 and 0.45%; thus, the deflocculant capacities of clays such as Sogamoso 1 and Sogamoso 2, as well as groups Ráquira and Cómbita (1, 4 and 5), are notable.

In summary, although it is not possible to establish a rigorous relationship between the results of the chemical analysis and the applicability of the clays, the clay minerals studied here have compositions that closely correspond to the technical classification of "ball clays";23,24 that is, common clays that contain an important fraction of kaolinite, chlorite, quartz and organic matter,25 without carbonates and with notable dispersion capacity.

### *3.2. Mineralogical Analysis*

The main clay minerals are kaolinite, smectite (initially montmorillonite), illite, chlorite, vermiculite and palygorskite.26,27,28 Because a clay is "a mixture", in different proportions, of some of these minerals, a direct way to establish a clay's identity and mineral content is through X-ray diffraction.29 Different minerals, by virtue of their purity, crystallographic orientation, crystal size and tectoid organization, present characteristic diffraction patterns that can even be used for quantitative effects.30,31

Figure 1 shows the diffractograms of the clays obtained in the Sogamoso region, Boyacá (Colombia). The most intense reflections, which stand out at 12.4 (plane 001), 24.8 (plane 002) and 67.7 degrees 2□, correspond to kaolin minerals;32 meanwhile, the signals located at 21.0, 26.6, 36.5, 39.4, 50.1, 59.8, and 68.1 2□ degrees indicate the presence of □–quartz,33 with a trigonal structure (space Group P3221, No. 154). The low intensity of kaolinite diffraction suggests a relatively small particle size, which, by virtue of its ability to incorporate water films, has an important degree of plasticity. With the exception of clay S1, which shows a reflection at 17.4 degrees 2□, suggesting the presence of smectites, the minerals from this provenance do not have appreciable amounts of expandable clays.

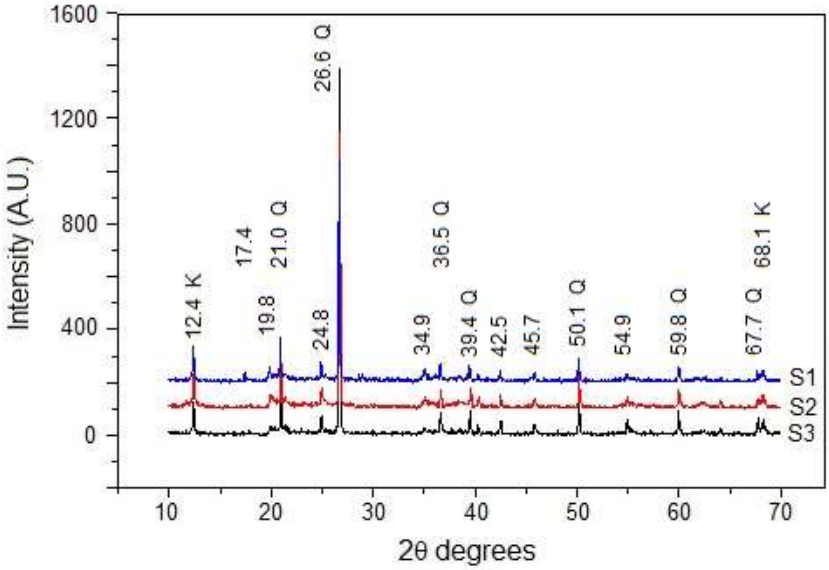


*Figure 1: Diffractograms of the Sogamoso clays (K = kaolinite, Q = a –quartz). S1 (blue) = Clay Sogamoso 1, S2 (red) = Clay Sogamoso 2, and S3 (black) = Clay Sogamoso 3. Reflections at 2 q angles are indicated.*

Figure 2 shows the X-ray diffraction patterns of clays collected in the municipality of Cómbita, Boyacá (Colombia). These minerals are characterized by the presence of kaolinite (reflection at 12.4 degrees 2 θ), α –quartz (with the most intense diffraction at 26.6 degrees 2 θ) and negligible contents of expandable clay minerals (smectites). In all cases, with signals at 27.4 (plane 110), 36.1 (plane 101) and 55.8 (plane 211) degrees 2 θ, the presence of TiO2 is evident, as indicated by the chemical analysis of the rutile variety, which is a thermodynamically stable polymorph.34 These results indicate that the presence of expandable clays from the smectite group is not evident; thus, the plastic characteristics of these clays are provided by kaolinite. From the point of view of mineralogical composition, S and C clays are similar; both minerals share the presence of kaolinite and the absence of smectites, although the rutile content is more notable in the C clays.

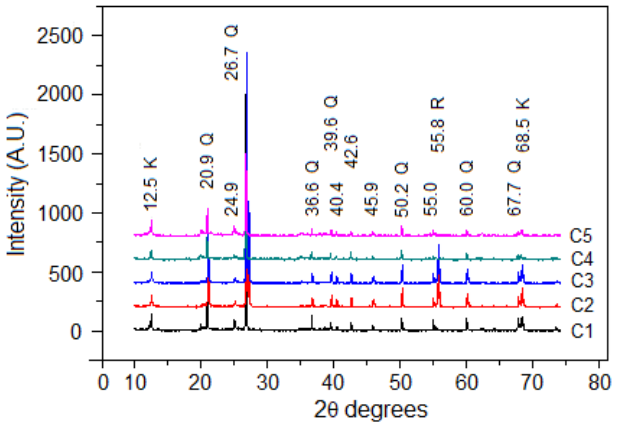


*Figure 2: Diffractograms of the Cómbita clays (K = kaolinite, Q = a–quartz, R = rutile). C1 (black) = Clay Cómbita 1, C2 (red) = Clay Cómbita 2, C3 (blue) = Clay Cómbita 3, C4 (green) = Clay Cómbita 4, and C5 = Clay Cómbita 5 (fuchsia). Reflections at 2q angles are indicated.*

Figure 3 shows the diffractograms of clays collected in the microbasin of the Ráquira River in the Department of Boyacá (Colombia). This region is made up of Cretaceous, Tertiary and Quaternary sedimentary rocks, composed of alluvial and colluvial deposits that are soft and poorly consolidated, which translate into sandy and shaly rocks such as claystones (laminar, siliceous, sandstones), mudstones and siltstones.[35] It is believed that the deposits of these clays come from the weathering processes of these sedimentary rocks.[36]

Like the Sogamoso and Cómbita clays, the Ráquira minerals are characterized by the notable presence of □–quartz. Here, kaolinite is the predominant clay mineral; however, the signals that arise at 19.9 (plane 002), 28.9 (plane 110) and 62.5 (plane 060) degrees 2□ suggest the presence of smectites, possibly montmorillonite and pyrophyllite.[37] The reflection located at 28.9 (plane 003) degrees 2□ also fits the pyrophyllite (plane 003).[38] The eventual presence of pyrophyllite, which is explained by the incorporation of silica into kaolinite, $Al_2(S_2O_5)(OH)_4 + SiO_2 \rightarrow Al_2(Si_4O_{10})(OH)_2 + H_2O$, tends to modulate the plasticity of clays owing to the low expansion coefficient and low deformation.[39,40]

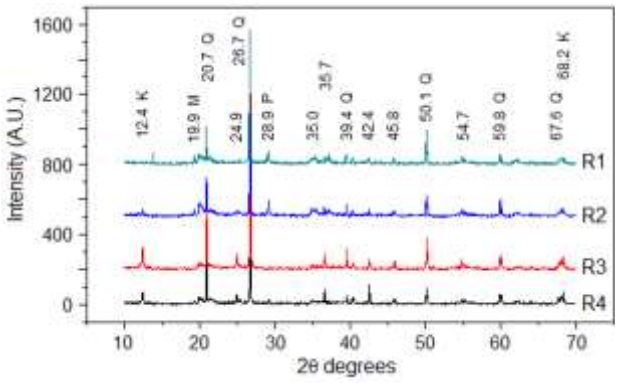


*Figure 3: Diffractograms of the Ráquira clays (K = kaolinite, Q = □–quartz, M = montmorillonite, P = pyrophyllite). R1 (green) = Clay Ráquira 1, R2 (blue) = Clay Ráquira 2, R3 (red) = Clay Ráquira 4, and R4 = Clay Ráquira 4 (black). Reflections at 2□ angles are indicated.*

### 3.3. Thermal Analysis

With few exceptions and due to their origin, secondary clay deposits are variable mixtures of different substances: hydrated phyllosilicates, silicates, different forms of water, silica (sand and quartz), alumina species, and organic matter. They also contain alkaline, alkaline earth ions and other metals that, arranged in the form of oxides, hydroxides or salts (halides, carbonates, sulfates and phosphates), make up heterogeneous systems. To examine the possible ceramic applications of such mixtures, which involve thermal treatments, it is necessary to evaluate their behavior with respect to temperature.

Figure 4 shows the thermograms (DTAs) obtained for raw clays from the Boyacá region (Colombia). The signals observed between 73 °C and 98 °C correspond to the loss of physi-adsorbed water, which is present in the different components of the raw clays: clay minerals, organic matter, silicon oxide, and metal oxides.[41] The bands observed between 175 °C and 187 °C are associated with the removal of adsorbed water contained in the interlaminar region of clay minerals.[42] No transitions are observed toward 130 °C; thus, the absence of smectites that may be stratified with kaolinite or illite is presumed. However, in Ráquira clay (R2), the 177 °C signal suggests the presence of bentonite, which is consistent with the mineralogical analysis. The peaks observed between 267 °C and 293 °C are due to the loss of coordinated water present in the exchangeable metal ions, the loss of interlaminar water and even the hydration water of some salts; however, for clays S2 (293 °C), C3 (274 °C), R2 (293 °C), and R4 (278 °C), the signal intensity is increased by the oxidation of organic matter. These bands may also correspond to the dehydration of Gibbsite.[43]

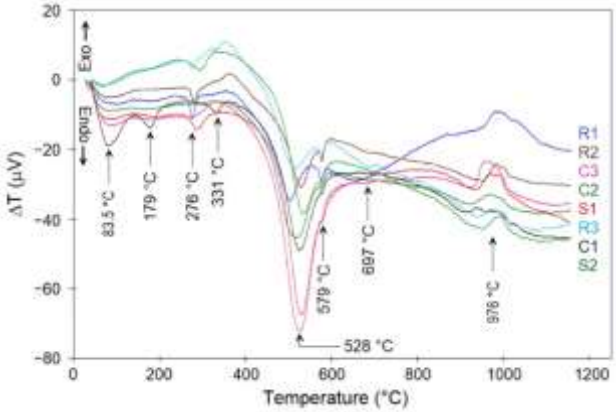


*Figure 4: Differential thermal analysis of clays from the Boyacá region (Colombia). From top to bottom: R1 (blue) = Clay Ráquira 1, R2 (brown) = Clay Ráquira 2, C3 (fuchsia) = Clay Cómbita 3, C2 (light green) = Clay Ráquira 2, S1 (red) = Clay Sogamoso 1, R3 (cyan) = Clay Ráquira 3, C1(black) = Clay Cómbita 1, and S2 (green) = Clay Sogamoso 2. The temperatures of the main transitions are highlighted.*

Some clays, such as C4, R3 and R4, present small endothermic bands between 331 °C and 372 °C that possibly correspond to the dehydroxylation of quartz. For all clays, the most intense transition is observed between 504 °C and 534 °C. This band is attributed to the dehydroxylation process of the clay: $Al_2Si_2O_5(OH)_4 \rightarrow Al_2Si_2O_7 + 2H_2O$.[44] The signal detected at 577 °C is due to the transition between kaolinite and metakaolin: $Al_2Si_2O_5(OH)_4 \rightarrow Al_2O_3.2SiO_2$ (amorphous Meta kaolinite) + $2H_2O$.[45] At 573 °C, the crystalline conversion of quartz also occurs: □–trigonal → □–hexagonal.

The endothermic signals that appear at approximately 684 °C are due to the dehydroxylation of smectites, when present, the decarboxylation of organic impurities and the decomposition of carbonates. The exothermic bands located between 774 °C and 807 °C are due to interactions between silica and different metal ions ($Na^+$, $K^+$, $Mg^{2+}$, $Ca^{2+}$, and $Fe^{3+}$) that form silicates. The peaks that arise between 856 °C and 972 °C correspond to the conversion of the □–hexagonal phase of quartz into tridymite and of metakaolin into silicon oxide spinels: $2Al_2Si_2O_7 \rightarrow 2Al_2O_3.3SiO_2 + SiO_2$.[46] Between 980 °C and 1000 °C, ceramic processes associated with the nucleation of pseudo mullite ($2Al_2O_3.3SiO_2 \rightarrow 2Al_2O_3.2SiO_2 + SiO_2$) are evident, which then transforms into mullite and cristobalite ($3Al_2O_3.SiO_2 \rightarrow 3Al_2O_3.SiO_2 + SiO_2$). Between 1017 °C and 1099 °C, to the extent that at 1150 °C the mullite phase grows,

quartz fusion, vitrification and sintering take place.[47]

Figure 5 shows the representative results of the thermogravimetric analysis of clays from the Boyacá region (Colombia). All the materials experienced mass loss at approximately 80 °C, an event that corresponds to the release of physically retained water. With the exception of the Cómbita 3 and Ráquira 3 samples, all the clays lose weight at 175 °C, which is associated with the loss of hydration water and the exit of interlaminar water.

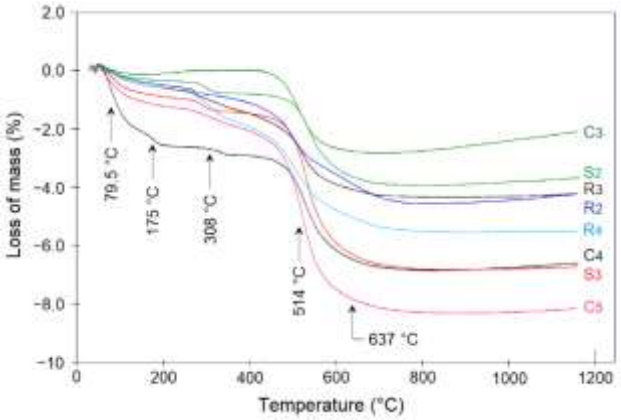


***Figure 5: Thermogravimetric analysis of clays from the Boyacá region (Colombia). From top to bottom: C3 (green) = Clay Cómbita 3, S2 (light green) = Clay Sogamoso 2, R3 (black) = Clay Ráquira 3, R2 (blue) = Clay Ráquira 2, R4 (cyan) = Clay Ráquira 4, S3 (red) = Clay Sogamoso 3, C5 (fuchsia) = Clay Cómbita 5. The main mass loses temperatures are indicated.***

Except for the Cómbita 3 clay, the different samples reported, at approximately 308 °C, experienced weight losses that fluctuated between 0.11% and 0.48%, which was attributed to the dehydroxylation of hydrated iron oxides (endothermic) and organic matter oxidation (exothermic).[48] Some clays, such as Cómbita 3 and Ráquira 4, present mass losses at approximately 372 °C, which are linked to the decomposition of organic matter.[49] For all clays, the greatest weight loss is observed at approximately 514 °C; the highest losses, 3.13% and 2.65%, corresponding to the Cómbita 5 and Sogamoso 3 clays, respectively. These mass losses are due to the dehydroxylation of kaolinite and other clays (montmorillonite and pyrophyllite) in the process of metakaolin formation.[50] For some clays (Cómbita 3, Ráquira 2 and Ráquira 4), mass loss at 637 °C stands out; these transitions are attributed to the transformation of quartz.[51]

### *3.4. Ceramic characterization*

The technological properties considered in the manufacturing process of porcelain stoneware tiles are linear contraction (LC), water absorption (WA), which accounts for open porosity, the expansion coefficient (LEC) and the presence of black heart (BH) in fired pieces.[52] Owing to their porosity, ceramic materials from clay (bricks, tiles, tiles, sanitary porcelain) can absorb liquid and gaseous substances and thereby modify certain characteristics, such as density, mechanical resistance, permittivity, conductivity and optical properties.[53] In another sense, to determine the firing temperatures, the temperature range in which the open porosity is zero, and the heat treatment conditions where the linear contraction is constant, which coincide with an optimal mechanical resistance, it is necessary to determine the water absorption capacity and linear shrinkage of fired ceramic bodies.[54, 55,56] In a gresification diagram, for a clay, which is considered a plastic material without additives or feldspars or silica derivatives, the sintering process (mullitization) is represented as a decrease in the water absorption capacity and modifications. Dimensional (shrinkage), compared to the firing temperature, typically advances above 1100 °C.[57]

Figure 6 shows the stoneware or vitrification obtained between 1090 °C and 1195 °C for samples made with clays from the Cómbita area in the Boyacá region (Colombia). For the C3 and C5 clays, the maximum contraction does not exceed 2.5%, which suggests a mineralogical composition based on nonexpandable minerals, whereas the contraction observed in C4 is greater. The trends in the water absorption capacity indicate that, for all cases, the open porosity tends to decrease with increasing thermal treatment, which is notable for C4 and very pronounced for C3 from 1165 °C, indicating a high degree of sintering.

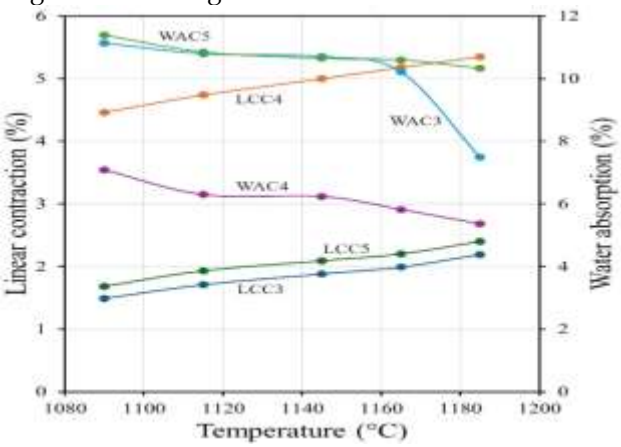


***Figure 6: Cómbita clays gresification diagram. Linear contraction: LCC3 (blue) = Clay Cómbita 3, LCC5 (green) = Clay Cómbita 5, LCC4 (orange) = Clay Cómbita 4. Water absorption: WAC4 (violet) = Clay Cómbita 4, WAC3 (cyan) (light green) = Clay***

***Cómbita 3, WAC4 = Clay Cómbita 4.***

Figure 7 shows the gresification diagram of clays from the Ráquira region, which are represented by a set of open-air deposits that have been exploited since pre-Columbian times and are used in the production of terracotta utensils. In all the cases, linear contraction increases gradually with temperature, being lower for clay R2, where the maximum contraction, at 1185 °C, is 2.2%, a situation that is combined with a water absorption capacity of only 4.4%, indicating the low open porosity and high sintering achieved by these clays. Although the greatest residual porosity and the greatest linear shrinkage are observed, R4 clay is also characterized by rapid sintering after 1165 °C; however, R3 clay not only shows greater linear shrinkage at higher temperatures but also has appreciable resistance to sintering above 1145 °C.

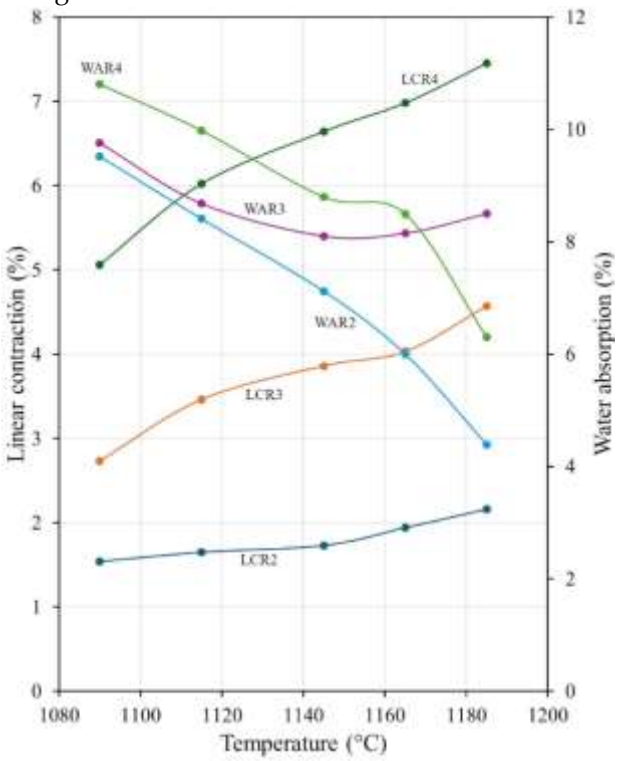


***Figure 7: Ráquira clays gresification diagram. Linear contraction: LCR2 (blue) = Clay Ráquira 2, LCR3 (orange) = Clay Ráquira 3, LCR4 (green) = Clay Ráquira 4. Water absorption: WAR2 (cyan) = Clay Ráquira 2, WAR3 (violet) = Clay Ráquira 3, WAR4 (light green) = Clay Ráquira 4.***

Figure 8 shows the stone formation curves (linear contraction and water absorption capacity) for the Sogamoso clays from the Boyacá region (Colombia). For clays S2 and S3, linear shrinkage increases linearly with temperature. For these clays, the calcination losses were 10.66% and 5.96%, respectively. According to the mineralogical analysis, both clays are expandable; which explains their behavior; however, the high sintering capacity of these minerals is notable, manifesting in a rapid decrease in water absorption.

These findings suggest that these minerals are refractory and that the sintering processes, owing to the mechanism of development of a viscous glassy phase, take place at relatively high temperatures. In other words, certain phenomena, such as the growth of the mullite phase and the dissolution of quartz, reduce the viscosity of the system and increase the firing temperature. Several of these diagrams are similar to those obtained for ceramic bodies produced by mixtures of clays from the Campos RJ region (Brazil), calcareous material and quartz.[58] The iron content in these materials was 9.1%, whereas the $Al_2O_3$ content was 27.9%, represented in kaolinite, illite and mica. The behavior of the diagram is attributed to the presence of $CaCO_3$, which produces CaO at 900 °C that reacts with metakaolin to promote the liquid phase.[59] Nevertheless, water absorption is relatively high and does not disappear below 1200 °C.

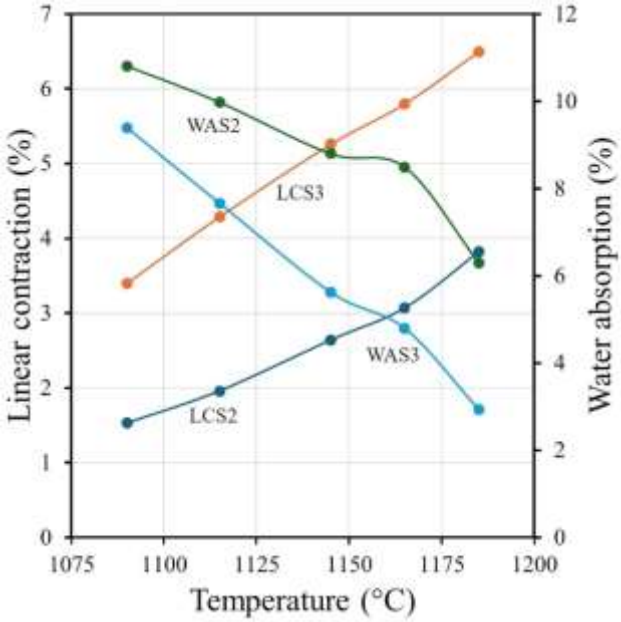


***Figure 8: Sogamoso clays gresification diagram. Linear contraction: LCS2 (blue) = Clay Sogamoso 2, LCS3 (orange) = Clay Sogamoso 3. Water absorption: WAS3 (cyan) = Clay Sogamoso 3, WAS3 (green) = Clay Sogamoso 3.***

In the temperature range studied, the behavior of the Sogamoso clays is similar to that of a clay that contains 18.8% $Al_2O_3$, 50.2% $SiO_2$, 7.8% $Fe_2O_3$, 3.2% CaO, and 3.9% MgO; the losses due to calcination were 11.0%, and the $TiO_2$ content was practically the same.[60] The clay contains kaolinite, illite, quartz and

dolomite, and the densification is explained by the presence of potassium, sodium and iron oxides, which promote the glassy phase. The idea is that the "mullitization" process is favored by the presence of $Fe^{3+}$ and that above 1050 °C, the quartz decreases, and the Si–Al spinel transforms into mullite and cristobalite.[61]

Although the clays studied reflect refractory properties of interest, owing to the kaolinite and quartz content, in general, the linear contraction behavior is stable, and the effect of gas evolution is not observed. The mechanical strength of crude oil was high, except for that of Ráquira 3 clay, which was 1.8 N $mm^{-2}$; in all cases, the plasticity indices were between 20.0% and 23.0%, which corresponds to liquid limits between 49.0% and 56.0% in the Casagrande plasticity chart, according to the Holtz–Kovacs diagram.[62,63,64] The absence of organic matter was notable in all materials.

The ceramic properties of fired clay bodies depend on the nature of the clay minerals, the mineralogy, the chemical composition, the particle size, the compaction or extrusion pressure, the green drying conditions, as well as on the calcination parameters (heating ramp), final temperature, residence time and atmosphere.[65,66] Studies based on response surface methodologies suggest that in a sintered ceramic body (stoneware type), water absorption should vary between 0.0% and 1.5%, whereas linear shrinkage should not exceed 13.0%.[67] In accordance with the ISO13006 technical standard, Cómbita 1 and 3 clays, and Ráquira 3 clays, vitrified ceramic bodies that are classified into groups BIb (Klinker) and AI and that correspond to tiles, have water absorption capacities. KLK and URS (red stoneware), with moduli of rupture close to 30 MPa. The remaining clays produce semi vitrified ceramic bodies that are classified into group BIIa, red stoneware, and GRS tiles with rupture moduli that range between 18 and 30 MPa.[68]

### *3.5. Coloring of Ceramic Bodies*

The fired color is a property that classifies ceramic tiles as white-body or red-body products. [69,70] The colorations reported correspond to data obtained through a spectrophotometer with a CIELAB measurement system, which classifies luminosity L (black to white), a (green to red), and b (blue to yellow).[71,72]

Figure 9 shows the coloration obtained for the fired Cómbita clay pieces, which are characterized by a brown coloration. The L coordinate decreases between 42 and 38, whereas the red and blue components decrease between 15 and 10. The resulting appearance resembles Pantone® color 7596C.

As suggested by the b coordinate, the yellow coloration increases in the Cómbita 1 and 4 clays. The reddish coloration of the clays and the derived ceramic bodies are attributed to the presence of hematite (□–$Fe_2O_3$), magnetite ($FeFe_2O_4$) and goethite (□–FeOOH).[73,74,75] Magnetite and goethite introduce yellow and brown colorations, although the yellow color is also due to the titanium oxide,[76,77] of the rutile variety.[78]

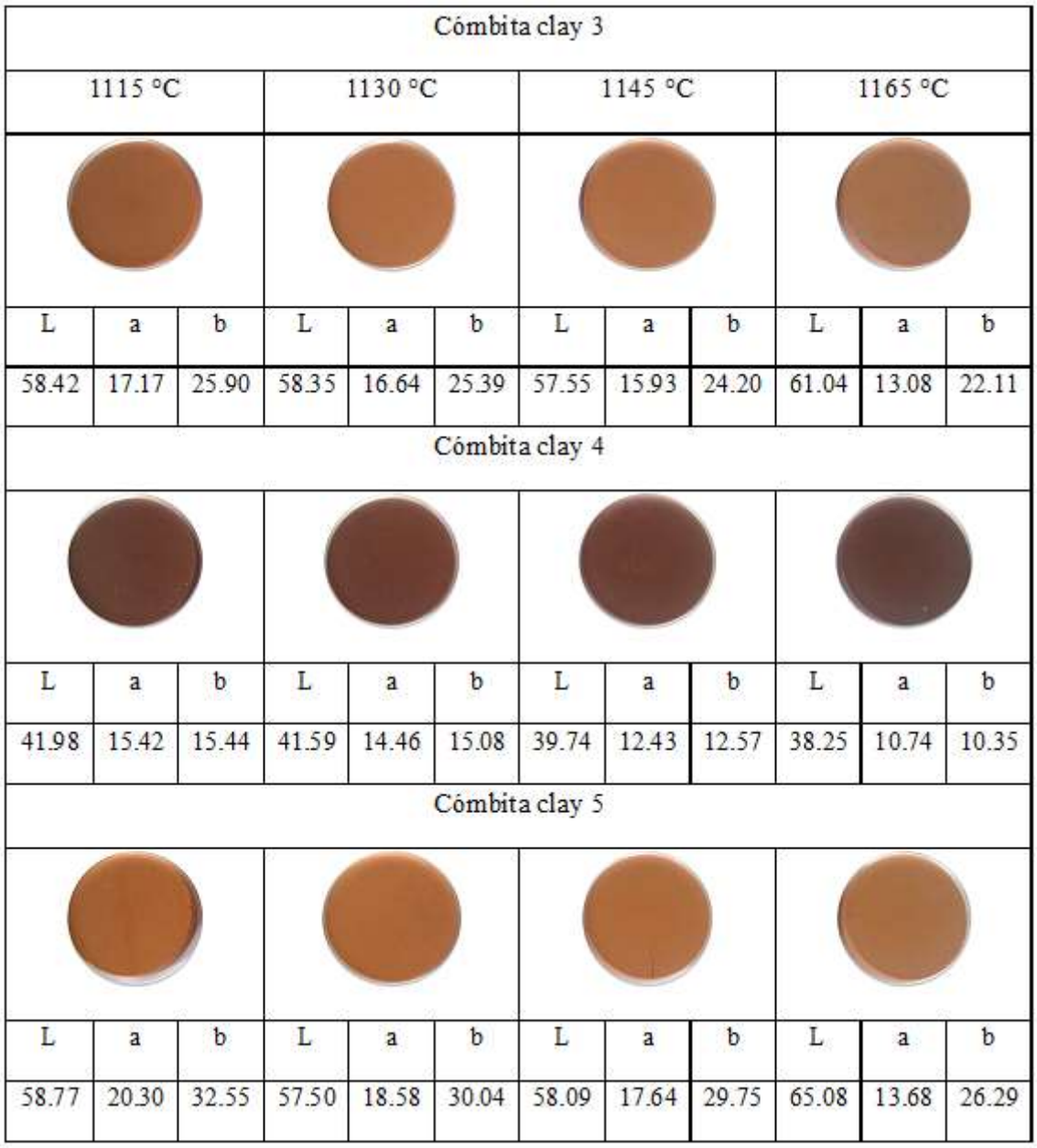

| Cómbita clay 3 | | | | | | | | | | | |
|---|---|---|---|---|---|---|---|---|---|---|---|
| 1115 °C | | | 1130 °C | | | 1145 °C | | | 1165 °C | | |
| L | a | b | L | a | b | L | a | b | L | a | b |
| 58.42 | 17.17 | 25.90 | 58.35 | 16.64 | 25.39 | 57.55 | 15.93 | 24.20 | 61.04 | 13.08 | 22.11 |
| **Cómbita clay 4** | | | | | | | | | | | |
| L | a | b | L | a | b | L | a | b | L | a | b |
| 41.98 | 15.42 | 15.44 | 41.59 | 14.46 | 15.08 | 39.74 | 12.43 | 12.57 | 38.25 | 10.74 | 10.35 |
| **Cómbita clay 5** | | | | | | | | | | | |
| L | a | b | L | a | b | L | a | b | L | a | b |
| 58.77 | 20.30 | 32.55 | 57.50 | 18.58 | 30.04 | 58.09 | 17.64 | 29.75 | 65.08 | 13.68 | 26.29 |

***Figure 9: CIELAB coloring of fired Cómbita clay pieces. L (luminosity) = whiteness, a = tendency toward red, b = yellow. The firing temperature is indicated at the top. 1 hour of cooking time.***

Figure 10 highlights that the white-fired ceramic body is represented by Ráquira 2 clay; the whiteness varies between 80 and 81, the red varies between 5 and 4, and the blue changes between 11 and 15, corresponding to a Pantone® 7500C color. Clays R3 and R4 leave a reddish color, compatible with Pantone® 7512 and 7517, respectively. The white firing of R1 clay is of great technological interest: consistent with its linear contraction and water absorption capacity (Figure 7), it constitutes an ideal raw material for producing porcelain stoneware.

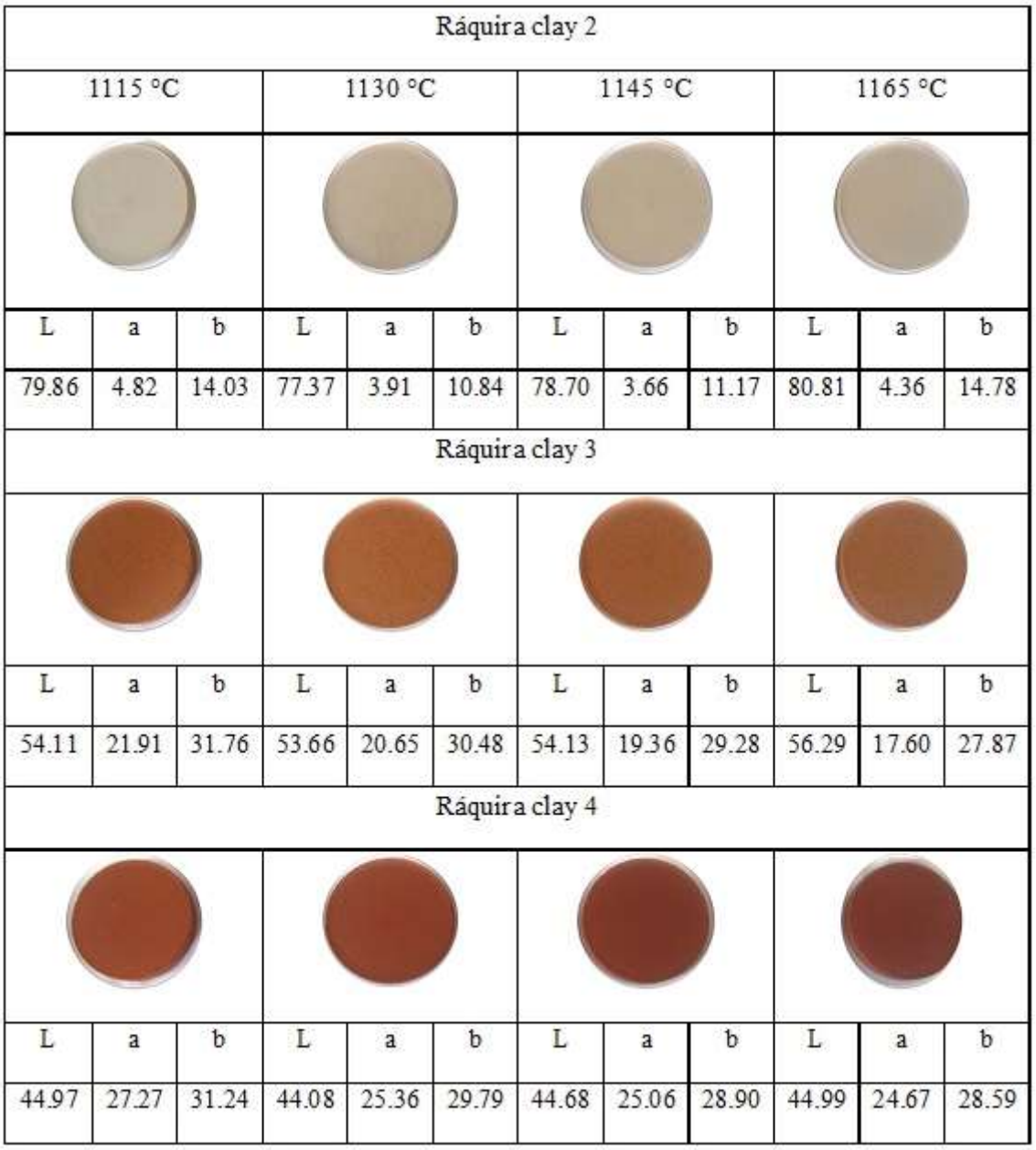


***Figure 10: CIELAB coloring of fired Ráquira clay pieces. L (luminosity) = whiteness, a = tendency toward red, b = yellow. The firing temperature is indicated at the top. 1 hour of cooking time.***

Figure 11 shows the coloration obtained during firing for test tubes made with the Sogamoso clays. Sogamoso 1 clay, treated between 1115 °C and 1165 °C, leaves a color with whiteness between 45 °C and 46 °C, a red color between 21 °C and 18 °C, and a blue color between 24 °C and 20 °C. In the Pantone® system, these coordinates are approximately 7600 °C in color. The rapid decrease in the water absorption capacity of clay S1, despite the relatively high contraction rate, suggests the use of this mineral as a raw material for the manufacture of red porous ceramics with good mechanical resistance.[79,80,81]

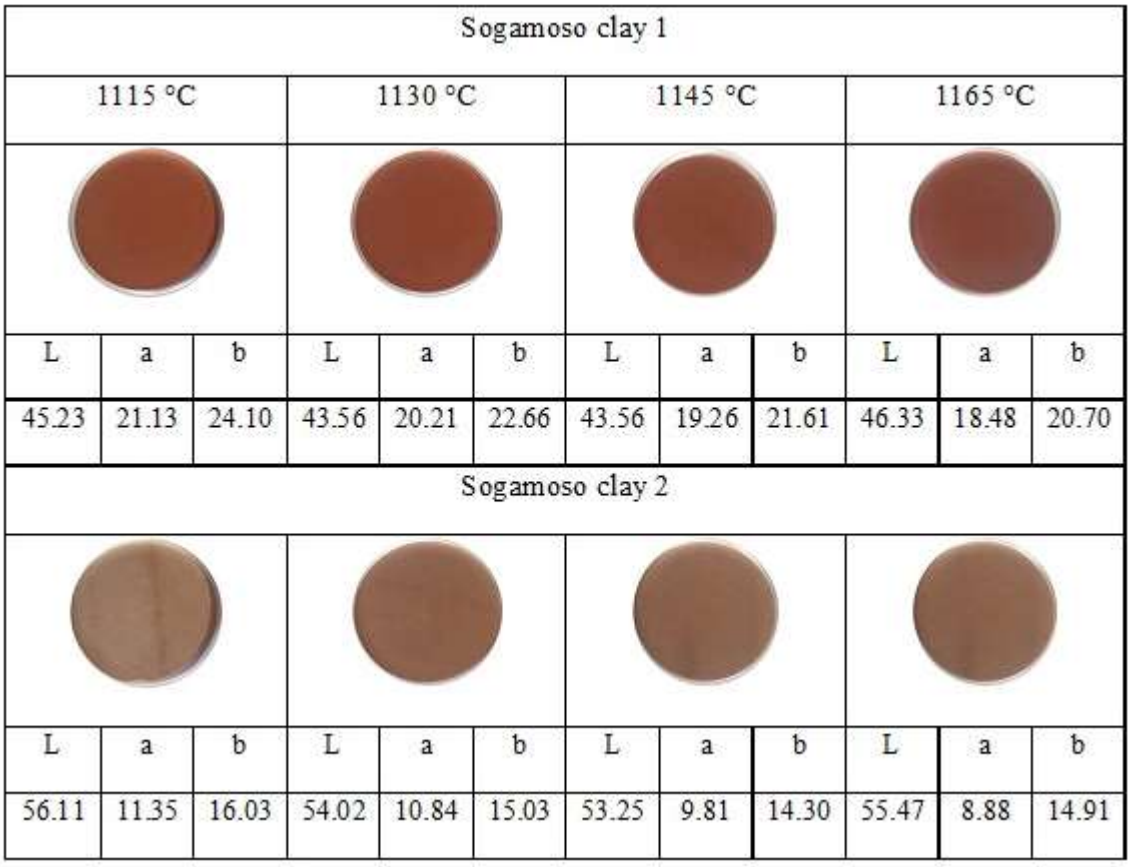

| Sogamoso clay 1 | | | | | | | | | | | |
|---|---|---|---|---|---|---|---|---|---|---|---|
| 1115 °C | | | 1130 °C | | | 1145 °C | | | 1165 °C | | |
| L | a | b | L | a | b | L | a | b | L | a | b |
| 45.23 | 21.13 | 24.10 | 43.56 | 20.21 | 22.66 | 43.56 | 19.26 | 21.61 | 46.33 | 18.48 | 20.70 |
| Sogamoso clay 2 | | | | | | | | | | | |
| L | a | b | L | a | b | L | a | b | L | a | b |
| 56.11 | 11.35 | 16.03 | 54.02 | 10.84 | 15.03 | 53.25 | 9.81 | 14.30 | 55.47 | 8.88 | 14.91 |

***Figure 11: CIELAB coloring of fired Sogamoso clay pieces. L (luminosity) = whiteness, a = tendency toward red, b = yellow. The firing temperature is indicated at the top. 1 hour of cooking time.***

Compared with the S1 mineral, which is fired reddish, the Sogamoso 2 clay shows a snowier coloration, with whiteness between 56 and 55 °C, a red color between 11 and 9 °C, and a blue color between 16 and 15 °C, for a Pantone® 7525C equivalent. This clay has a lower content of pigment oxides, among which $Fe_2O_3$ stands out at 2.45%, and losses due to calcination of 10.66% have been reported. The mineralogical analysis indicates the presence of expandable clays, meaning the addition of some components that improve the structural geometry, such as quartz, sodium feldspar, and degreasers, makes this raw material optimal for producing porcelain stoneware. [82,83] None of the test pieces examined had a black heart.

## 5. CONCLUSIONS

The mineralogical analysis of the materials indicates the presence of quartz and clay minerals (kaolinite); for the clays originating from Ráquira, the presence of montmorillonite, pyrophyllite and feldspar stands out. The physicochemical analysis of the different clays highlights variations in the alumina content and gives them a markedly kaolinitic character.

Considering the gresification diagrams, the studied clays behave adequately for use as components in paste formulations for traditional ceramics, such as red porous, white porous, porcelain stoneware and red stoneware, intended for the manufacture of ceramic wall tiles and floors.

The mixtures of these clays, such as Ráquira 2 and Sogamoso 2, in certain proportions can be used to formulate high-quality ceramic pastes (high degree of sintering and mechanical resistance); however, depending on the type of product for which they are intended, other raw materials must be added, such as carbonates, feldspars, calcites and kaolins, which are also present in the Boyacá region, Colombia.

**Acknowledgments:** The authors thank the Universidad Nacional de Colombia, the Universidad Pedagógica y Tecnológica de Colombia (Tunja), the Boyacá Regional Mining Center of SENA (Sogamoso), the Universitat

Jaume I de Castelló (Spain), the Escola Superior de Ceràmica de L'Alcora (Spain), and the company Tierra Atomizada, S. A. (Spain) for their support in the collection, preparation and physicochemical characterization of the minerals. The authors also express their gratitude to and recognition of the engineer D. Enrique Cerisuelo (R.I.P.), the chemist D. José Planas and Dr. Esther Barrachina, for their support in interpreting the results and providing permanent advice.

**Author contributions:** N. E. Céspedes Prieto verified the sample collection, chemical analyses and ceramic characterization; J. Llop Pla carried out the thermal analyses and paste formulation; J. S. Valencia Ríos worked on the mineralogical characterization; and J. B. Carda Castelló provided the conceptual framework of the research and studied the ceramic behavior of clays.

## REFERENCES

1. Clark, Sh. R.; *Asian Perspect.* **2003**, *42*, 304. [Crossref]
2. Tsetlin, Y. B.; *J. Hist. Archaeol. Anthropol. Sci.* **2018**, *3*, 209. [Crossref]
3. Twiss, K. C.; *J. Anthropol. Archaeol.* **2008**, *27*, 418. [Crossref]
4. Montana, G.; *Archaeol. Anthropol. Sci.* **2020**, *12*, 175. [Crossref]
5. Kennedy, D.; *J. Polit. Econ.* **1927**, *35*, 522. [Crossref]
6. de Pablo, L.; *B. Soc. Geol. Mex.* **1964**, *27*, 49. [Crossref]
7. Díaz Rodríguez, L. A.; Torrecillas, R., *Bol. Soc. Esp. Ceram. V.* **2002**, *41*, 459. [Crossref]
8. Aboudi Mana, S. Ch.; Hanafiah, M. M.; Khan Chowdhury, A. J.; *Geol. Ecol. Landsc.* **2017**, *1*, 155. [Crossref]
9. Wilson, M. J.; *Clay Miner.* **1999**, *34*, 7. [Crossref]
10. Konta, J.; *Appl. Clay Sci.* **1995**, *10*, 275. [Crossref]
11. Zvyagin, B. B.; *Clay. Clay Miner.* **2001**, *49*, 642. [Crossref]
12. Ndlovu, B.; Farrokhpay, S.; Bradshaw, D.; *Int. J. Miner. Process.* **2013**, *125*, 149. [Crossref]
13. Sánchez, E.; García–Ten, J.; Sanz, V.; Moreno, A., *Ceram. Int.* **2010**, *36*, 831. [Crossref]
14. Moreno-Maroto, J. M.; Alonso-Azcárate, J.; *Appl. Clay Sci.* **2018**, *161*, 57. [Crossref]
15. Waterkemper Vieira, A.; de Mello Innocentini, M. D.; Mendes, E.; Gomes, Th.; Demarch, A.; Klegues Montedo, O. R.; Angioletto, E.; *Mater. Res.* **2017**, *20*, 637. [Crossref]
16. Arkame, Y.; Harrati, A.; Imgirne, A.; Moustapha, A.; Et-Tayea, Y.; Yamari, I.; Sdiri, A.; El Bouari, A.; Sadik, Ch.; *Open Ceram.*, **2024**, *18*, 100591. [Crossref]
17. Haigh, S. K.; Vardanega, P. J.; Bolton, M. D.; *Géotechnique* **2013**, *63*, 435. [Crossref]
18. Landrou, G.; Brumaud, C.; Plötze, M. L.; Winnefeld, F.; Habert, G.; *Colloid. Surface. A* **2018**, *539*, 252. [Crossref]
19. Romagnoli, M.; Andreola, F., *J. Eur. Ceram. Soc.* **2007**, *27*, 1871. [Crossref]
20. Shu, Z.; García–Ten, J.; Monfort, E.; Amorós, J. L.; Zhou, J.; Wang, Y. X., *Ceram. Int.* **2012**, *38*, 517. [Crossref]
21. Farrokhpay, S.; Morris, G. E.; Britcher, L. G.; *Miner. Eng.* **2012**, *39*, 39. [Crossref]
22. Castellini, E.; Berthold, Ch.; Malferrari, D.; Bernini, F.; *Appl. Clay Sci.* **2013**, *83–84*, 162. [Crossref]
23. Galos, K.; *Ceram. Int.* **2011**, *37*, 851. [Crossref]
24. Carty, W. M.; Senapati, U.; *J. Am. Ceram. Soc.* **1998**, *81*, 3. [Crossref]
25. Wattel-Koekkoek, E. J. W.; van Genuchten, P. P. L.; Buurman, P.; van Lagen, B.; *Geoderma* **2001**, *99*, 27. [Crossref]
26. Murray, H. H.; *Clay Miner.* **1999**, *34*, 39. [Crossref]
27. Zhang, D.; Zhou Ch., H.; Lin Ch., X.; Tong, D. Sh.; Yu, W. H.; *Appl. Clay Sci.* **2010**, *50*, 1. [Crossref]
28. Uddin, F.; *Metall. Mater. Trans. A* **2008**, *39A*, 2804. [Crossref]
29. Zhou, X.; Liu, D.; Bu, H.; Deng, L.; Liu, H.; Yuan, P.; Du, P.; Song, H.; *Solid Earth Sci.* **2018**, *3*, 16. [Crossref]
30. Alves, M. E.; Mascarenhas, Y. P.; French, D. H.; Vaz, C. P. M.; *Aust. J. Soil Res.* **2007**, *45*, 224. [Crossref]
31. Prandel, L. V.; Saab, S. C.; Brinatti, A. M.; Giarola, N. F. B.; Leite, W. C.; Cassaro, F. A. M.; *Radiat. Phys. Chem.* **2014**, *95*, 65. [Crossref]
32. Andrini, L.; Gauna, M. R.; Conconi, M.S.; Suárez, G.; Requejo, F. G.; Aglietti, E. F.; Rendtorff, N. M.; *Appl. Clay Sci.* **2016**, *124–125*, 39. [Crossref]
33. Götze, J.; *Mineral. Mag.* **2009**, *73*, 645. [Crossref]
34. Okada, K.; Yamamoto, N.; Kameshima, Y.; Yasumori, A.; *J. Am. Ceram. Soc.* **2001**, *84*, 1591. [Crossref]
35. Erguler, Z. A.; Shakoor, A.; *Eng. Geol.* **2009**, *108*, 36. [Crossref]
36. Zhao, T.; Xu, Sh.; Hao, F.; *Earth Sci. Rev.* **2023**, *246*, 104598. [Crossref]

37. Serpa Guarino, A. W.; San Gila, R. A. S.; Polivanov, H.; Menezes, S. M. C.; *J. Brazil. Chem. Soc.* **1997**, *8*, 581. [Crossref]
38. Sánchez Soto, P. J.; Pérez Rodríguez, J. L.; *Bol. Soc. Esp. Ceram. V*. **1998**, *37*, 285. [Crossref]
39. Pérez-Maqueda, L. A.; Montes, O. M.; González-Macías, E. M., Franco, F.; J. Poyato; Pérez-Rodríguez, J. L.; *Appl. Clay Sci.* **2004**, *24*, 201. [Crossref]
40. Ali, M. A.; Ahmed, H. A. M.; Ahmed, H. M.; Hefni, M.; *Appl. Sci.* **2021**, *11*, 11357. [Crossref]
41. Rat, E.; Martínez–Martínez, S.; Sánchez-Garrido, J. A.; Pérez–Villarejo, L.; Garzón, E.; Sánchez–Soto, P. J.; *Ceram. Int.* **2023**, *29*, 14814. [Crossref]
42. Alfonso, P.; Penedo, L. A.; García–Valles, M.; Martínez, S.; Martínez, A.; Trujillo, J. E.; *J. Therm. Anal. Calorim.* **2022**, *147*, 5413. [Crossref]
43. Plante, A. F.; Fernández, J. M.; Leifeld, J.; *Geoderma* **2009**, *153*, 1. [Crossref]
44. Gasparini, E.; Tarantino, S. C.; Ghigna, P.; Riccardi, M. P.; Cedillo-González, E. I.; Siligardi, C.; Zema, M.; *Appl. Clay Sci.* **2013**, *80–81*, 417. [Crossref]
45. Daou, I.; Lecomte–Nana, G. L.; Tessier–Doyen, N.; Peyratout, C.; Gonon, M. F.; Guinebretiere, R.; *Minerals* **2020**, *10*, 480. [Crossref]
46. Wang, S.; Gainey, L.; Mackinnon, I. D. R.; Allen, Ch.; Gu, Y.; Xi, Y.; *J. Build. Eng.* **2023**, *66*, 105802. [Crossref]
47. Lee, W. E.; Souza, G. P.; McConville, C. J.; Tarvornpanich, T.; Iqbal, Y.; *J. Eur. Ceram. Soc.* **2008**, *28*, 465. [Crossref]
48. Kawigraha, A.; Soedarsono, W.; Harjanto, S.; Pramusanto; *Adv. Mat. Res.* **2013**, *774-776*, 682. [Crossref]
49. Kristl, M.; Muršec, M.; Šuštar, V.; Kristl, J.; *J. Therm. Anal. Calorim.* **2016**, *123*, 2139. [Crossref]
50. Ptáček, P.; Frajkorová, F.; Šoukal, F.; Opravil, T.; *Powder Technol.* **2014**, *264*, 439. [Crossref]
51. Ríos, S.; Salje, E. K. H.; Redfern, S. A. T.; *Eur. Phys. J. B* **2001**, *20*, 75. [Crossref]
52. Pérez, J. M.; Romero, M.; *Ceram. Int.*, **2014**, *40*, 1365. [Crossref]
53. Romero, M.; Pérez, J. M.; *Mater. Construcc.* **2015**, *65*, e065. [Crossref]
54. Lee, V. G.; Yeh, T. H.; *Mater. Sci. Eng. A* **2008**, *485*, 5. [Crossref]
55. Cargnin, M.; Ulson de Souza, S. M. A. G; Ulson de Souza, A. A.; de Noni Jr., A.; *Braz. J. Chem. Eng.* **2015**, *32*, 433. [Crossref]
56. Sánchez-Soto, P. J.; Eliche-Quesada, D.; Martínez-Martínez, S.; Pérez-Villarejo, L.; Garzón, E.; *Materials* **2022**, *15*, 583. [Crossref]
57. Vasić, M. V.; Pesoc, L.; Vasić, M. R.; Mijatović, N.; Mitrić, M.; Radojević, Z.; *Bol. Soc. Esp. Ceram. V*. **2022**, *61*, 241. [Crossref]
58. Sousa, S. J. G.; Holanda, J. N. F.; *Ceram. Int.* **2005**, *31*, 215. [Crossref]
59. Kłosek-Wawrzyna, E.; Małolepszya, J.; Murzyn, P.; *Procedia Eng.* **2013**, *57*, 572. [Crossref]
60. Carbajal, L.; Rubio-Marcos, F.; Bengochea, M. A.; Fernández, J. F.; *J. Eur. Ceram. Soc.* **2007**, *27*, 4065. [Crossref]
61. Yamuna, A.; Devanarayanan, S.; Lalithambika, M.; *J. Am. Ceram. Soc.* **2002**, *85*, 1409. [Crossref]
62. Ribeiro, M. J.; Ferreira, J. M.; Labrincha, J. A.; *Ceram. Int.* **2005**, *31*, 515. [Crossref]
63. Andrade, F. A.; Al-Qureshi, H. A.; Hotza, D.; *Appl. Clay Sci.* **2011**, *51*, 1. [Crossref]
64. Bukhary, A.; Azam, Sh.; *Geotechnics* **2023**, *3*, 744. [Crossref]
65. Murad, E.; Wagner, U.; *Hyperfine Interact.* **1998**, *117*, 337. [Crossref]
66. Souza, G. P.; Sánchez, R.; de Holanda, J. N. F.; *Cerâmica* **2002**, *48*, 102. [Crossref]
67. Zanelli, C.; Raimondo, M.; Guarini, G.; Dondi, M.; *J. Non-Cryst. Solids* **2011**, *357*, 3251. [Crossref]
68. Zanatta, T.; Antunes Boca Santa, R. A.; Padoin, N.; Soares, C.; Gracher Riella, H.; *J. Mater. Res. Technol.* **2021**, *11*, 121. [Crossref]
69. Ferrari, S.; Gualtieri, A. F.; *Appl. Clay Sci.* **2006**, *32*, 73. [Crossref]
70. He, H.; Yue, Q.; Qi, Y.; Gao, B.; Zhao, Y.; Yu, H.; Li, J.; Li, Q.; Wang, Y.; *Appl. Clay Sci.* **2012**, *70*, 67. [Crossref]
71. Martirena, F.; Almenares, R.; Zunino, F.; Alujas, A.; Scrivener, K., *RILEM Tech. Lett.* **2020**, *5*, 1. [Crossref]
72. Wiśniewska, K.; Pichór, W.; Kłosek-Wawrzyn, E.; *Materials* **2021**, *14*, 6380. [Crossref]
73. Walter, D.; *Thermochim. Acta* **2006**, *445*, 195. [Crossref]
74. Legodi, M. A.; de Waal, D.; *Dyes Pigments* **2007**, *74*, 161. [Crossref]
75. Ristić, M.; Opačak, I.; Musić, S.; *J. Alloys Compd.* **2013**, *559*, 49. [Crossref]
76. Gázquez, M. J.; Bolívar, J. P.; García-Tenorio, R.; Vaca, F.; *Mater. Sci. Appl.* **2014**, *5*, 441. [Crossref]
77. Z. Mesíková; P. Šulcová; M. Trojan; *J. Therm. Anal. Calorim.* **2006**, *83*, 561. [Crossref]
78. Gargori, C.; Cerro, S.; Galindo, R.; G. Monrós; *Ceram. Int.* **2010**, *36*, 23. [Crossref]
79. Valanciene, V.; Siauciunas, R.; Baltusnikaite, J., *J. Eur. Ceram. Soc.* **2010**, *30*, 1609. [Crossref]

80. Alves Pinto, L.; Delmondes de Souza, Th.; Bernardes Silva, D.; Pinheiro Peixoto, L.; Brasileiro Rodrigues, M. I., *Rev. Materia* **2021**, *26*, 13019. [Crossref]
81. Silva, K. R.; Menezes, R. R.; Campos; L. F. A.; Santana, L. N. L., *Cerâmica* **2022**, *68*, 270. [Crossref]
82. Dondi, M.; Raimondo, M.; Zanelli, C., *Appl. Clay Sci.* **2014**, *96*, 91. [Crossref]
83. García-Ten, J.; Dondi, M.; Vieira Lisboa, J. V. M. B.; Vicent Cabedo, M.; Pérez-Villarejo, L.; Rambaldi, E.; Zanelli, Ch.; *Sust. Mater. Technol.* **2024**, *39*, e00832. [Crossref]